Drug Design, Development and Therapy

Dovepress
Taylor & Francis Group

Open Access Full Text Article

ORIGINAL RESEARCH

Exploratory Study on the Role of Emodin in Alleviating MPTP-Induced Neurotoxicity: A Focus on p53-Ferroptosis Signaling

Yujun Chen[1,2,*], Yuhang Zhao[1,2,*], Qing Wang[1,2], Qiuchi Chen[3], Xiqun Chen[1,2], Kai Yang[1,2]

[1]Department of Integrative Medicine, Huashan Hospital, Fudan University, Shanghai, People's Republic of China; [2]Institute of Integrative Medicine, Fudan University, Shanghai, People's Republic of China; [3]Department of Radiology, Affiliated Hospital of Nanjing University of Chinese Medicine, Nanjing, 210029, People's Republic of China

*These authors contributed equally to this work

Correspondence: Xiqun Chen; Kai Yang, Department of Integrative Medicine, Huashan Hospital, Fudan University, Shanghai, People's Republic of China, Email chen_xiqun@fudan.edu.cn; kyang19@fudan.edu.cn

Background: Parkinson's disease (PD) is a common neurodegenerative disorder. Emodin (EMD), which is derived from multiple Chinese medicinal herbs, has been reported to possess anti-inflammatory, anti-ferroptosis, and neuroprotective effects. However, the mechanisms underlying the regulation of PD-related ferroptosis remain unclear.

Objective: To investigate whether EMD protects dopaminergic neurons in 1-methyl-4-phenyl-1,2,3,6-tetrahydropyridine (MPTP)-induced models of PD and to elucidate its underlying mechanisms.

Methods: Potential EMD targets were predicted using SEA and Swiss databases. The PD targets were identified using the OMIM and GeneCards databases. Overlapping genes were introduced to construct protein-protein interactions (PPI) and perform Gene Ontology (GO) and Kyoto Encyclopedia of Genes and Genomes (KEGG) analyses. Molecular docking was used to ascertain the possibility of the binding of EMD to p53 and TfR1. The stability of EMD-p53 complex was validated by using molecular dynamics simulations using the YASARA. To validate these mechanisms, we used an MPTP-induced mouse model to investigate the beneficial effects of EMD. Motor function was assessed using the open field and rotarod tests. Malondialdehyde (MDA) and iron contents in the midbrain were determined. SH-SY5Y cells were subjected with 1-methyl-4-phenyl-pyridinium (MPP^+) or ferroptosis inducer. Ferroptosis signaling, iron metabolism, and mitochondrial superoxide levels were investigated using Western blotting, qPCR, immunofluorescence, and flow cytometry.

Results: Enrichment analysis revealed that the shared targets of the PD and EMD gene sets were involved in iron metabolism, with TP53 being the most connected protein in the PPI network. Molecular docking analysis suggested that EMD formed a stable complex with p53 or TfR1. Molecular Dynamics Simulation further confirmed that the interactions between EMD and p53 remained stable over time. In vivo studies demonstrated the beneficial effects of EMD in an MPTP mouse model of PD. This action was achieved by inhibiting p53 expression and mitigating ferroptosis signaling in the substantia nigra (SN). EMD similarly attenuated cell injury and ferroptosis in SH-SY5Y cells by inhibiting p53-ferroptosis signaling. In contrast, pharmacological enhancement of p53 nullified these effects in the MPP^+-treated SH-SY5Y cells.

Conclusion: These preliminary results indicate that EMD could exert neuroprotective effects against MPTP-induced toxicity, possibly via modulating p53-ferroptosis signaling.

Keywords: emodin, neurodegeneration, MPTP, Parkinson's disease, ferroptosis, p53

Introduction

Parkinson's disease (PD) is a common neurodegenerative disorder.[1] PD is characterized by progressive degeneration of dopaminergic neurons (DaN) in the substantia nigra (SN), leading to hallmark motor symptoms.[2] Current treatments for

Received: 8 March 2025
Accepted: 24 July 2025
Published: 1 December 2025

Graphical Abstract

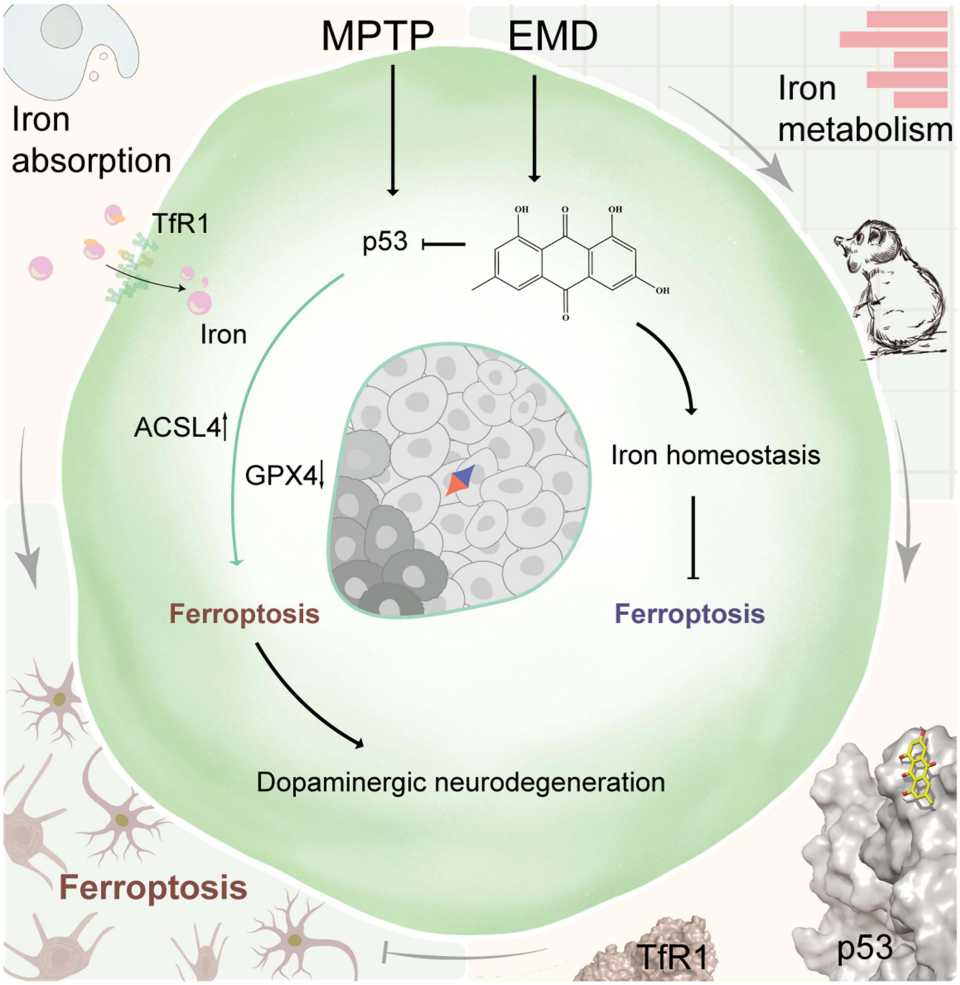

PD are largely limited to replacing dopamine levels and activating dopamine receptors. These therapeutics fail to halt degenerative progression.[3] Consequently, there is an urgent need to develop novel therapeutic strategies for PD.

Ferroptosis is a unique mechanism of iron-dependent regulated cell death characterized by altered iron homeostasis, accumulation of lipid peroxides, and imbalanced oxidative defense.[4] The protein transferrin receptor 1 (TfR1), encoded by transferrin receptor (TFRC), and Solute Carrier Family 11 member 2 (SLC11A2), plays a key role in cellular iron import and influences systemic iron homeostasis.[5] Iron accumulation in the brain worsens with age and is considered a hallmark of PD.[6] It is documented that neurons acquire most of their iron via the transferrin-TfR1 system.[7] Neurons regulate iron levels by minimal sequestration or efficient export via Ferroportin1 (FPN).[8] Although TfR1 is broadly involved in iron uptake, its upregulation has been reported in various ferroptosis models, suggesting it may contribute to ferroptosis susceptibility by promoting intracellular iron accumulation.[9] Acyl-CoA synthetase long-chain family member 4 (ACSL4), an enzyme esterifying CoA into specific polyunsaturated fatty acids, may trigger phospholipid peroxidation and induce ferroptosis.[10] Inhibition of ACSL4 may reduce lipid peroxides and ameliorate PD.[11] Glutathione peroxidase 4 (GPX4) is a key suppressor of ferroptosis.[12] Abnormal iron accumulation in the SN and elevated oxidative stress are key pathological features of PD.[8,13] In a 1-methyl-4-phenyl-1,2,3,6-tetrahydropyridine (MPTP) induced mouse model, midbrain exhibits dysregulation iron metabolism, increased ACSL4 expression and impaired GPX4 activity.[14] These

findings highlight the contribution of ferroptosis to PD progression and the therapeutic potential of targeting ferroptosis-related pathways.

The p53 protein, encoded by the tumor protein p53 (TP53, or p53) gene, has been appeared to be a highly attractive target for anti-cancer research.[15] TP53 is recognized as a tumor suppressor and executes its diverse functions, including cellular cycle arrest, DNA damage repair, metabolic homeostasis, cell senescence, autophagy, and apoptosis.[16] Various researches have implicated recently that p53 has an association with ferroptosis.[17] Cardiomyocytes challenged by doxorubicin exhibits iron overload and lipid peroxide accumulation in a p53-dependent manner.[18] The activation of p53 results in iron homeostasis dysregulation through increasing TfR1 expression.[18] Importantly, emerging studies have shown that p53-mediated ferroptosis may be involved in neuronal death in PD models, suggesting that p53 is a potential contributor to neurodegeneration via ferroptosis pathways.[19,20] Targeting the p53-ferroptosis signaling shows promise for PD treatment.

Emodin (EMD), a natural anthraquinone compound, is derived from multiple Chinese medicinal herbs including Cassia obtusifolia, Aloe vera, Polygonum cuspidatum, Polygonum multiflorum, and Rheum palmatum.[21] Emerging evidences show that EMD confers various beneficial actions, including anti-bacterial, anti-inflammatory, anti-ferroptosis and neuroprotective effects.[22] It is reported that EMD has a beneficial effect on various neurodegenerative diseases, including PD and Alzheimer's disease.[22] Although recent researches suggest EMD has positive effects on neuroprotection via a wide range of biological targets, its role in controlling neurodegenerative diseases and its pharmacological mechanism of action require further elucidation.

Here, we hypothesized that p53 inhibition-mediated regulation of ferroptosis signaling is the primary pharmacological mechanism of EMD. We explored whether EMD protects against dopaminergic neurodegeneration and clarified whether the beneficial effects of EMD are associated with p53-ferroptosis signaling inhibition.

Materials and Methods

Materials and Reagents

Stock solutions of 10 mM EMD (Selleck Chemicals, S2295, Purity: 99.75%), 400 mM 1-methyl-4-phenylpyridinium (MPP^+, Aladdin, N137206), 10 mM RSL3 (Med Chem Express, HY-100218A), 1 mM Erastin (Med Chem Express, HY-15763) in DMSO, and 50 mM C16-Ceramide (C16, MCE, HY-100354) in ethanol were used. We prepared small aliquots (30 μL) of each drug and stored them at −20°C. For the cell experiments, the stock solutions were diluted to a specific concentration of 2 mM for MPP^+, 3 μM for RSL3, 5 μM for Erastin, and 50 μM for C16.

The Cell Counting Kit-8 (CCK-8), Lipid Peroxidation malondialdehyde (MDA) Assay Kit, and MPTP were obtained from Beyotime Biotechnology (Shanghai, China). The Cell Total Iron Colorimetric Assay Kit was obtained from Elabscience (Wuhan, China). MitoSOX Red was purchased from MedChem Express (Shanghai, China). FerroOrange was purchased from Dojindo (Kumamoto, Japan). Antibodies against anti-TfR1, anti-ACSL4, anti-GPX4, anti-FPN, anti-FTH1, anti-β-Actin, anti-TH, anti-LPCAT3, and Alexa Fluor 594-labeled secondary antibody were purchased from Abclonal Technology Co., Ltd. (Wuhan, China). The anti-p53 antibody was obtained from Cell Signaling Technology (Danvers, MA, USA).

Obtaining Potential Targets of EMD and PD

The Canonical SMILES of EMD, available on PubChem (https://pubchem.ncbi.nlm.nih.gov/), was imported into the similarity ensemble approach (SEA, https://sea.bkslab.org/) and Swiss Target Prediction (Swiss, http://www.swisstargetprediction.ch/) to predict the EMD-related targets. Potential targets of Parkinson's disease (PD) were identified using online Mendelian inheritance in Man (OMIM, https://www.omim.org/) and the GeneCards database (http://www.genecards.org/). We focused on the intersection between the two gene sets for subsequent analysis.

Network Construction and Enrichment Analysis

Overlapping genes for EMD and PD targets were introduced into the STRING database (https://cn.string-db.org/) to construct protein-protein interactions (PPI). The Cytoscape software (version 3.11.0) was used to create a visual network.

For Gene Ontology (GO) and Kyoto Encyclopedia of Genes and Genomes (KEGG) pathway enrichment analyses, gene lists containing 91 shared targets were entered into a Database for Annotation, Visualization, and Integrated Discovery (DAVID, https://david.ncifcrf.gov/). The results were visualized using R package.

Molecular Docking

Autodock4 software was employed to ascertain the binding possibility of EMD with the core proteins p53 (PDB ID: 8DC6) and TfR1 (PDB ID: 6Y76) for docking simulation. PyMOL 2.6.0 was employed to adjust the protein molecules, including removing water molecules and extraneous ligands and adding hydrogen atoms. AutoDock Tools 1.5.6, was used to simulate molecular docking. Finally, the results were visualized using PyMOL version 2.6.0.

Molecular Dynamic (MD) Simulation

YASARA Structure software was employed to perform molecular dynamics simulation in 80 ns running time. The Root-Mean-Square Deviation (RMSD) and Root-Mean-Square Fluctuation (RMSF) results were used for assessing structural stability.

Cell Culture

The human SH-SY5Y neuroblastoma cell line was procured from Procell Life Science & Technology Co., Ltd. (Wuhan, China). The cells were cultivated in DMEM/F12 (Gibco, USA) supplemented with 10% fetal bovine serum (Gibco, USA) and 1% streptomycin-penicillin solution (Beyotime, China) and maintained at 37°C in a 5% CO_2 incubator. Cells were seeded at a density of 5×10^5 cells/well in 6-well plates pre-treated with poly-D-lysine (Beyotime, China), followed by co-culturing with EMD (2 μM, 5 μM, and 10 μM), MPP^+ (2 mM), and C16 (50 μM) for 12 h in the RT-qPCR assay and for 24 h in other assays.

Cell Viability Assay

The CCK-8 assay was conducted to analyze the viability of SH-SY5Y cells treated with various concentrations of EMD (1–80 μM). The cells were incubated at 37°C for 1 h, followed by treatment with 10% CCK-8. The absorbance was measured at 450 nm using a SpectraMax i3x microplate reader (Molecular Devices, CA, USA).

Animal Modeling and Treatment

All animal procedures used in this study were conducted in compliance with the guidelines of the Animal Experimental Ethics Committee of Shanghai Medical School, Fudan University, China (Approval Number: 202411013Z). C57BL/6J mice (10 weeks old, male, 24–26 g) were purchased from Shanghai Jihui Laboratory Animal Care Co., Ltd. (Shanghai, China) and kept under the specific pathogen-free conditions that controlled a 12h light/dark cycle at a temperature of 22–23°C. To generate an acute MPTP model, mice were randomly divided into four groups according to body weight: normal control group (CON, n = 12), MPTP model group (MPTP, n = 12), low-dose EMD treatment group (MPTP + EMDL, 50 $mg.kg^{-1}$ i.g. EMD, n = 12), and high-dose EMD treatment group (MPTP + EMDH, 100 $mg.kg^{-1}$ i.g. EMD, n = 12). The EMD treatment groups were administered the corresponding doses once daily for eight days. Subsequently, the mice were intraperitoneally administered MPTP at a dose of 20 $mg.kg^{-1}$ body weight on the sixth day after EMD administration. The CON group received an equivalent volume of normal saline. After the behavioral tests, the mice were euthanized.

Behavioral Tests

To evaluate spontaneous locomotor activity and coordination ability of the mice, open-field and rotarod tests were conducted. The mice were trained for adaptive exercise for two days prior to the test. For the open field test, a SuperFlex open field system (40 × 40×40 cm; Omnitech Electronics Inc. Columbus, OH) was employed for 3 min to monitor mouse activity, and fusion system software (Omnitech Electronics, Inc.) was used to capture the animals' real-time position and quantify locomotor parameters. For the rotarod test, mice were placed on the rotarod and the speed was set from 20 to 30 rpm for 1 min. The time at which the mice fell from the rod and the total distance were recorded.

Western Blotting

Whole-protein extracts from SH-SY5Y cells and SN of mice were initially separated by 10% SDS-PAGE and then transferred to PVDF membranes equilibrated with ethanol. The membranes were blocked with 5% bovine albumin for 1 h and subsequently probed with primary antibodies against anti-p53 (1:1000 dilution), anti-TfR1 (1:1000 dilution), anti-ACSL4 (1:1000 dilution), anti-GPX4 (1:1000 dilution), anti-TH (1:1000 dilution), anti-LPCAT3 (1:1000 dilution), anti-FPN (1:1000 dilution), anti-FTH1 (1:1000 dilution), anti-β-Actin (1:50,000 dilution) at 4°C overnight, followed by HRP-labeled secondary antibodies (1:5000 dilution) for 1 h at room temperature. The protein bands were detected using Bio-Rad Image Lab Touch software and analyzed using ImageJ software. The final protein expression levels were normalized to that of β-Actin.

RT-qPCR Assay

Total RNA from mouse SN and SH-SY5Y cells was extracted using a SteadyPure Universal RNA Extraction Kit (Accurate Biology, Hunan, China). First-strand cDNA was synthesized and subjected to quantitative real-time PCR (qRT-PCR) analysis using SYBR Green Pro Taq HS Mix (Accurate Biology, Hunan, China). Data were analyzed on a QuantStudio 6 Flex system (Applied Biosystems, USA) using the $2^{-\Delta\Delta Ct}$ method. β-Actin was used to normalize gene expression values. The primer sequences used are listed in Table 1.

Table 1 The Sequences of Primer in RT-qPCR Assay

Gene		Sequence
hACSL4	Forward Primer	CATCCCTGGAGCAGATACTCT
	Reverse Primer	TCACTTAGGATTTCCCTGGTCC
hGPX4	Forward Primer	GAGGCAAGACCGAAGTAAACTAC
	Reverse Primer	CCGAACTGGTTACACGGGAA
hNRF2	Forward Primer	TCAGCGACGGAAAGAGTATGA
	Reverse Primer	CCACTGGTTTCTGACTGGATGT
hLPCAT3	Forward Primer	GGAGCTGAGCCTTAACAAGTT
	Reverse Primer	CAAAGCAAAGGGGTAACCCAG
hTFRC	Forward Primer	ACCATTGTCATATACCCGGTTCA
	Reverse Primer	CAATAGCCCAAGTAGCCAATCAT
hFPN	Forward Primer	CTACTTGGGGAGATCGGATGT
	Reverse Primer	CTGGGCCACTTTAAGTCTAGC
hFTH1	Forward Primer	CCCCCATTTGTGTGACTTCAT
	Reverse Primer	GCCCGAGGCTTAGCTTTCATT
hSLC11A2	Forward Primer	TGGAGATCATGGGGAGTCTG
	Reverse Primer	AAGAAAACCTGGTCCGGTGAA
hTP53	Forward Primer	CAGCACATGACGGAGGTTGT
	Reverse Primer	TCATCCAAATACTCCACACGC
hβ-Actin	Forward Primer	CCTTCCTTCCTGGGCATGG
	Reverse Primer	GATCTTCATTGTGCTGGGTGC
mACSL4	Forward Primer	CCTGAGGGGCTTGAAATTCAC
	Reverse Primer	GTTGGTCTACTTGGAGGAACG
mGPX4	Forward Primer	TGTGCATCCCGCGATGATT
	Reverse Primer	CCCTGTACTTATCCAGGCAGA
mSLC7A11	Forward Primer	GGCACCGTCATCGGATCAG
	Reverse Primer	CTCCACAGGCAGACCAGAAAA

(*Continued*)

https://doi.org/10.2147/DDDT.S522381

Table 1 (Continued).

Gene		Sequence
mLPCAT3	Forward Primer	GACGGGGACATGGGAGAGA
	Reverse Primer	GTAAAACAGAGCCAACGGGTAG
mTFRC	Forward Primer	GTTTCTGCCAGCCCCTTATTAT
	Reverse Primer	GCAAGGAAAGGATATGCAGCA
mFPN	Forward Primer	TGGAACTCTATGGAAACAGCCT
	Reverse Primer	TGGCATTCTTATCCACCCAGT
mFTH1	Forward Primer	CAAGTGCGCCAGAACTACCA
	Reverse Primer	ACAGATAGACGTAGGAGGCATAC
mβ-Actin	Forward Primer	GGCTGTATTCCCCTCCATCG
	Reverse Primer	CCAGTTGGTAACAATGCCATGT

Immunohistochemistry (IHC)

For IHC staining, the mice brain paraffin sections were prepared and incubated with anti-TH (1:200 dilution) overnight at 4°C, followed by incubation with an HRP-conjugated secondary antibody. DAB reagent was used for visualization. The sections were then counterstained with hematoxylin. Finally, images were photographed using a scanning microtome (KF-FL-005, KFBIO, China).

Midbrain MDA and Iron Content Determination

Midbrain samples were homogenized by sonication, followed by centrifugation at 12,000 × g for 10 min. The supernatants were collected for subsequent analyses. The lipid Peroxidation MDA Assay Kit and Cell Total Iron Colorimetric Assay Kit were used to assay midbrain MDA and iron content, following the manufacturer's instructions.

Intracellular Superoxide Assay

Superoxide levels were measured using MitoSOX Red (MedChem Express, Shanghai, China), following the manufacturer's instructions. Briefly, SH-SY5Y cells were washed with PBS and stained with 5 μM MitoSOX Red reagent for 30 min in an incubator at 37°C. The cells were then rinsed with PBS for 3 times. Images were captured at a wavelength of 594 nm using an ImageXpress Pico scanner (Molecular Devices, USA).

Immunofluorescence Staining

For Immunofluorescence analysis, SH-SY5Y cells were fixed in 10% formalin and prepared to incubate with a primary antibody overnight at 4°C, followed by incubation with Alexa Fluor 594-labeled secondary antibodies for 1 h at room temperature. The cells were counterstained with DAPI (2 $\mu g.mL^{-1}$, Yeasen, Shanghai, China). Images were acquired using an ImageXpress Pico scanner (Molecular Devices).

Flow Cytometry

SH-SY5Y cells were collected after treatment with MPP^+ and EMD followed by digestion in a single-cell suspension. The harvested cells were treated with 1 μM FerroOrange for 30 min in an incubator at 37°C. Flow cytometric analysis was performed using an Attune NxT Flow Cytometer (Life Technologies). The data were analyzed using Flowjo v10.8.1 software.

Result Presentation

All data are presented as the mean ± SEM. Due to the exploratory nature of this study and the limited sample size (n=3–4), no formal statistical comparisons were performed. The results are intended to describe observed trends and generate hypotheses for future validation.

Results

Network Pharmacology Identifies the Targets of EMD in the Treatment of PD

The chemical structure of EMD is shown in Figure 1A. In total, 11,791 PD-related genes were identified from the OMIM and GeneCards databases, and 117 potential targets of EMD were predicted using the Swiss and SEA databases. Ninety-one therapeutic targets were identified by intersecting these two gene sets (Figure 1B). The PPI network showed that TP53 had the highest number of connections (114), suggesting that TP53 is likely the key target of EMD (Figure 1B). GO enrichment analysis highlighted pathways such as iron ion binding, $NADP^+$ activity, mitochondrial function, and reactive oxygen species (ROS) metabolism (Figure 1C). Similarly, KEGG enrichment analysis identified pathways including the p53 signaling

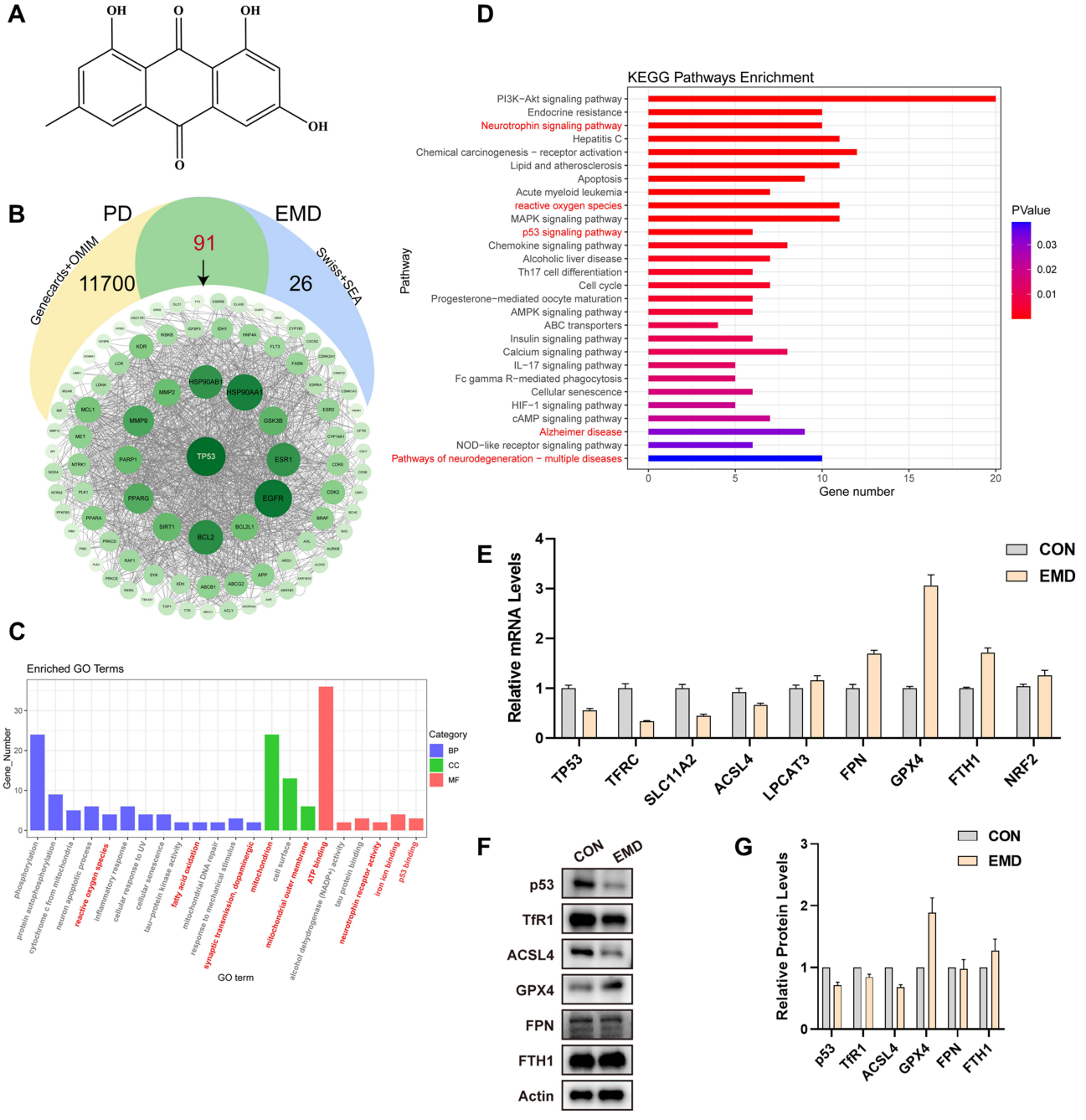

Figure 1 Network pharmacology explores the targets of EMD in the treatment of PD. (**A**) The structure of EMD. (**B**) The PPI network of the overlapped genes between EMD and PD. (**C**) KEGG enrichment analysis of the overlapped genes. (**D**) GO enrichment analysis of the overlapped genes. (**E**) Relative mRNA levels of ferroptosis-related genes in SH-SY5Y cells (n=3). (**F** and **G**) Western blot assay validated that EMD effectively depressed the expression of ferroptosis-related protein in SH-SY5Y cells (n=3).

https://doi.org/10.2147/DDDT.S522381

pathway, Alzheimer's disease, and pathways of neurodegeneration involving multiple diseases (Figure 1D). These findings suggest that EMD may exert anti-oxidative stress and anti-ferroptosis effects, highlighting its potential as a therapeutic agent for neurodegenerative diseases. To verify the above results, SH-SY5Y cells were treated with EMD for 24 h and the expression of ferroptosis-related genes and proteins was collected. The results showed that EMD reduced the expression of TP53, TFRC, SLC11A2, and ACSL4, while upregulating the expression of FPN, GPX4, and FTH1 (Figure 1E). Similarly, EMD reduced the protein expression of p53, TfR1, and ACSL4 while increasing GPX4 levels (Figure 1F and G). However, FPN expression did not increase significantly after EMD treatment, but FTH1 expression showed a slight increase (Figure 1F and G). These results suggest that EMD exerts anti-ferroptosis effects and alleviates dopaminergic neurodegeneration.

EMD Ameliorates MPTP-Induced Dyskinesia and Dopaminergic Neuronal Damage in Mice

To explore the neuroprotective effects of EMD, we evaluated the behavioral and neural status of MPTP-induced mice following EMD treatment. The in vivo experimental design timeline is shown in Figure 2A. Body weight decreased after

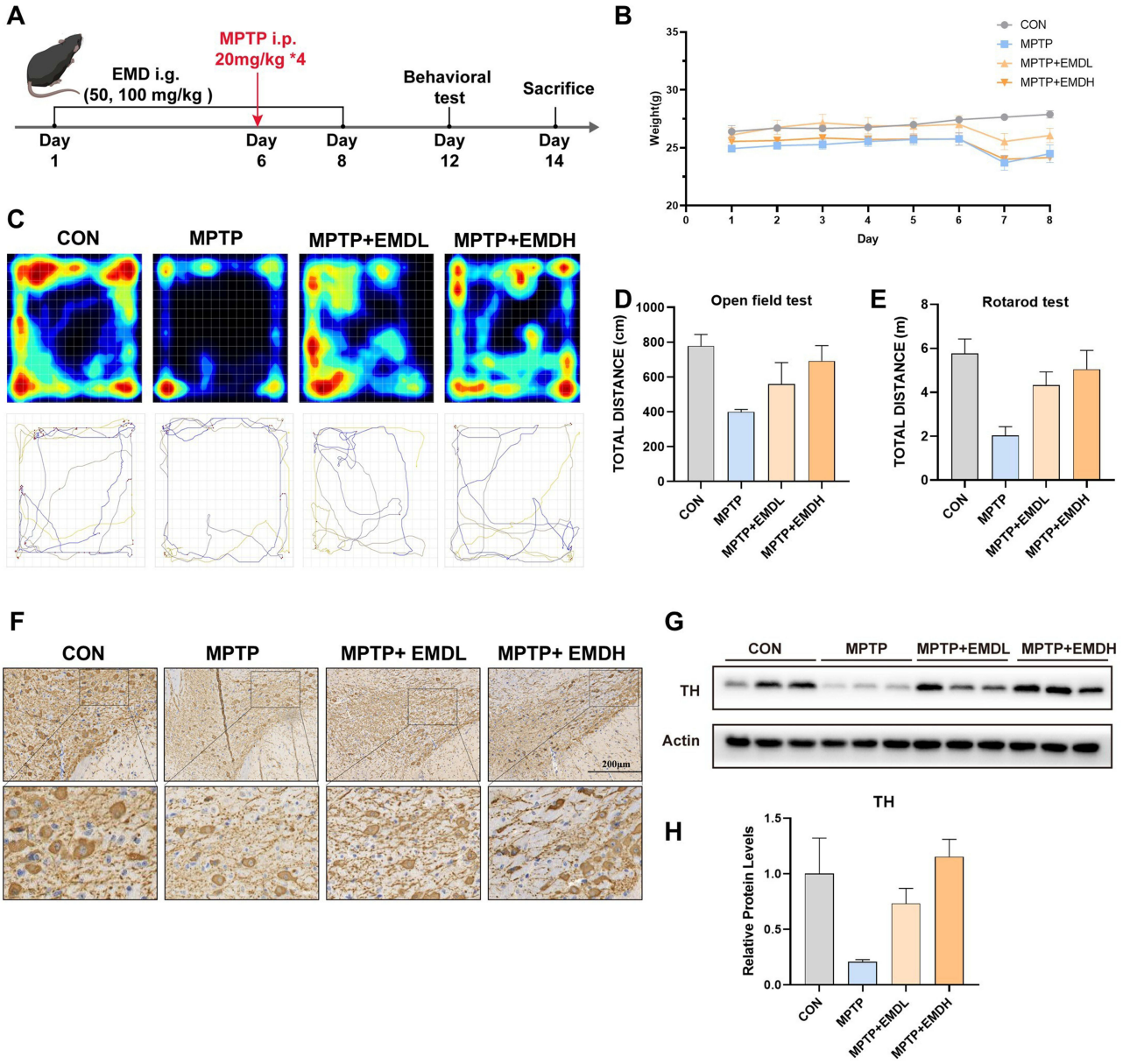

Figure 2 EMD ameliorates dyskinesia and dopaminergic neuronal damage in mice. (**A**) Schedule and timeline for the experimental design in vivo. (**B**) The change of body weight during the animal experiment. (**C** and **D**) Representative movement images and total distance in the open field test. (**E**) Total distance in the rotarod test. (**F**) Immunohistochemistry for TH in the SN of mice. Scale bars: 200 μm. (**G** and **H**) Western blot assay validated that EMD effectively protected against MPTP-induced DaN damage.

MPTP intervention, whereas the high-dose EMD group showed alleviated weight loss (Figure 2B). Motor behavior was evaluated using the open field and rotarod tests. MPTP treatment significantly induces hypokinesia. The total distance decreased in both the open field test and rotarod test, and the changes were rescued by high-dose EMD administration (Figure 2C–E). TH, the rate-limiting enzyme for dopamine synthesis, is the hallmark of DaN.[23] Mice subjected to MPTP administration displayed a decrease in the number of DaN in the SN and the level of the TH protein. EMD treatment mitigated these changes in a dose-dependent manner (Figure 2F–H). Collectively, these findings indicate that EMD exerts neuroprotective effects against MPTP-induced neural damage.

EMD Rescues the Dysregulation of p53 and Curbs the Ferroptosis in vivo

Ferroptosis has been regarded as one of the critical factors contributing to neurodegeneration in PD, and the inhibition of ferroptosis may have therapeutic potential.[24] While measuring the expression of ferroptosis-related genes, we observed that MPTP increased the levels of TFRC, ACSL4 and LPCAT3 in the SN, but did not affect the gene expression levels of SLC11A2, GPX4, FTH1 and SLC7A11. However, the high-dose EMD group exhibited lower TFRC, ACSL4, and LPCAT3, and higher GPX4 and FTH1 mRNA expression (Figure 3A–G). Additionally, MPTP treatment induced higher midbrain MDA and ferric ion levels than in the CON group (Figure 3H and I). This finding suggests that an imbalance between iron homeostasis and lipid peroxidation occurs in the SN. Conversely, EMD treatment reduced the changes in midbrain MDA and iron contents (Figure 3H and I). Similarly, ferroptosis-related protein analysis showed increases in p53, TfR1, and ACSL4 levels along with decreased GPX4 expression. However, EMD treatment mitigated these alterations to varying extents (Figure 3J–O). These results indicate that EMD counteracted ferroptosis in MPTP-treated mice.

EMD Attenuates Ferroptosis Induced by MPP+ in SH-SY5Y Cells

Subsequently, we assessed whether EMD attenuated ferroptosis in MPP^+-induced SH-SY5Y cells. According to CCK8 results, EMD (10 μM) did not affect cell viability (Figure 4A). Both RSL3 and Erastin, ferroptosis inducers that impair cell survival, were relieved by EMD intervention (Figure 4B and C). Furthermore, EMD suppressed the overaccumulation of ROS in SH-SY5Y cells subjected to MPP^+ insult (Figure 4D and E). These findings suggest that EMD can ameliorate oxidative damage in cells. Meanwhile, the TfR1 immunofluorescence assay showed that EMD reduced TfR1 expression compared with that in the MPP^+ group (Figure 4D and E). Additionally, flow cytometry analysis of FerroOrange showed that EMD reversed MPP^+-induced ferrous iron accumulation (Figure 4F). These results indicate that EMD treatment prevents MPP^+ induced ferrous iron accumulation and ferroptosis in vitro.

EMD Rescues the Dysregulation of p53 and Curbs the Ferroptosis in vitro

Given the observed effects of EMD on the regulation of cell iron content and ferroptosis, we investigated the mechanisms of EMD in vitro. In line with the findings obtained from the mouse SN, we confirmed that MPP^+ had an impact on the expression of TFRC and ACSL4 (Figure 5A and B). EMD treatment relieved these alterations in gene expression to varying degrees (Figure 5A and B). EMD treatment relieved the exacerbated gene expression of TP53 induced by MPP^+ exposure (Figure 5C). These findings were further validated by detection of cellular ferroptosis-related protein expression (Figure 5D–I). MPP^+ exposure increased the protein expression of p53, TfR1, ACSL4, and LPCAT3, and decreased GPX4 expression, which was prevented by EMD treatment (Figure 5D–I). Collectively, these results suggest that EMD counteracts ferroptosis induced by MPP^+.

The Activation of p53 Curbs EMD Inhibiting MPP+-Triggered Ferroptosis in SH-SY5Y Cells

The binding energy of the small molecule EMD and the proteins (p53 and TfR1) were calculated by Autodock4, resulting in values of −3.28 and −5.15 kcal/mol, respectively. Molecular docking revealed that EMD possibly interacted with p53 and TfR1 (Figure 6A). The RMSD remained within 2–4 Å, suggesting a stable complex structure throughout the simulation (Figure 6B). Most residues showed minimal fluctuation (Figure 6C). Subsequently, we verified whether EMD-

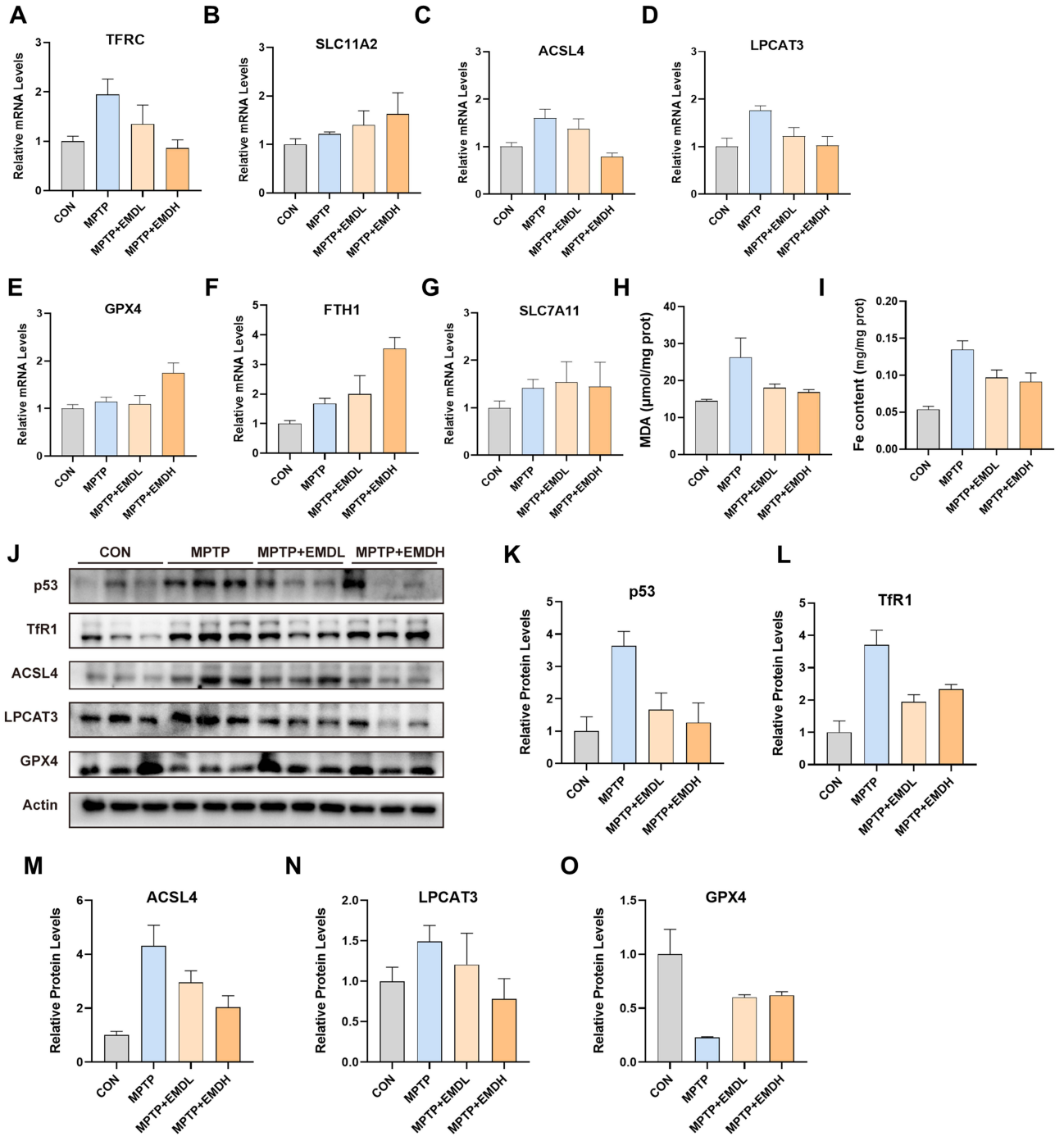

Figure 3 EMD rescues the dysregulation of p53 and curbs the ferroptosis in vivo. (**A**–**G**) Relative mRNA levels of ferroptosis-related genes in MPTP-induced mice. (**H**) The assay of MDA content in MPTP-induced mice midbrain. (**I**) The assay of iron content in MPTP-induced mice midbrain. (**J-O**) Western blot assay validated that EMD effectively rescued the dysregulation of p53 and inhibited the ferroptosis in mice midbrain.

induced p53 downregulation mediated ferroptosis inhibition under MPP^+/MPTP-induced conditions. C16, a selective p53 activator, was used to activate p53 signaling in vitro. EMD reduced TFRC and ACSL4 gene expression in SH-SY5Y cells exposed to MPP^+. Nevertheless, this suppressive action was attenuated when the cells were co-cultured with C16 (Figure 6D and E). Furthermore, C16 exposure exacerbated the dysregulation of p53, TfR1, and ACSL4 proteins in SH-SY5Y cells induced by MPP^+ (Figure 6F–I), but it almost invalidated the inhibitory effect of EMD on MPP^+-mediated

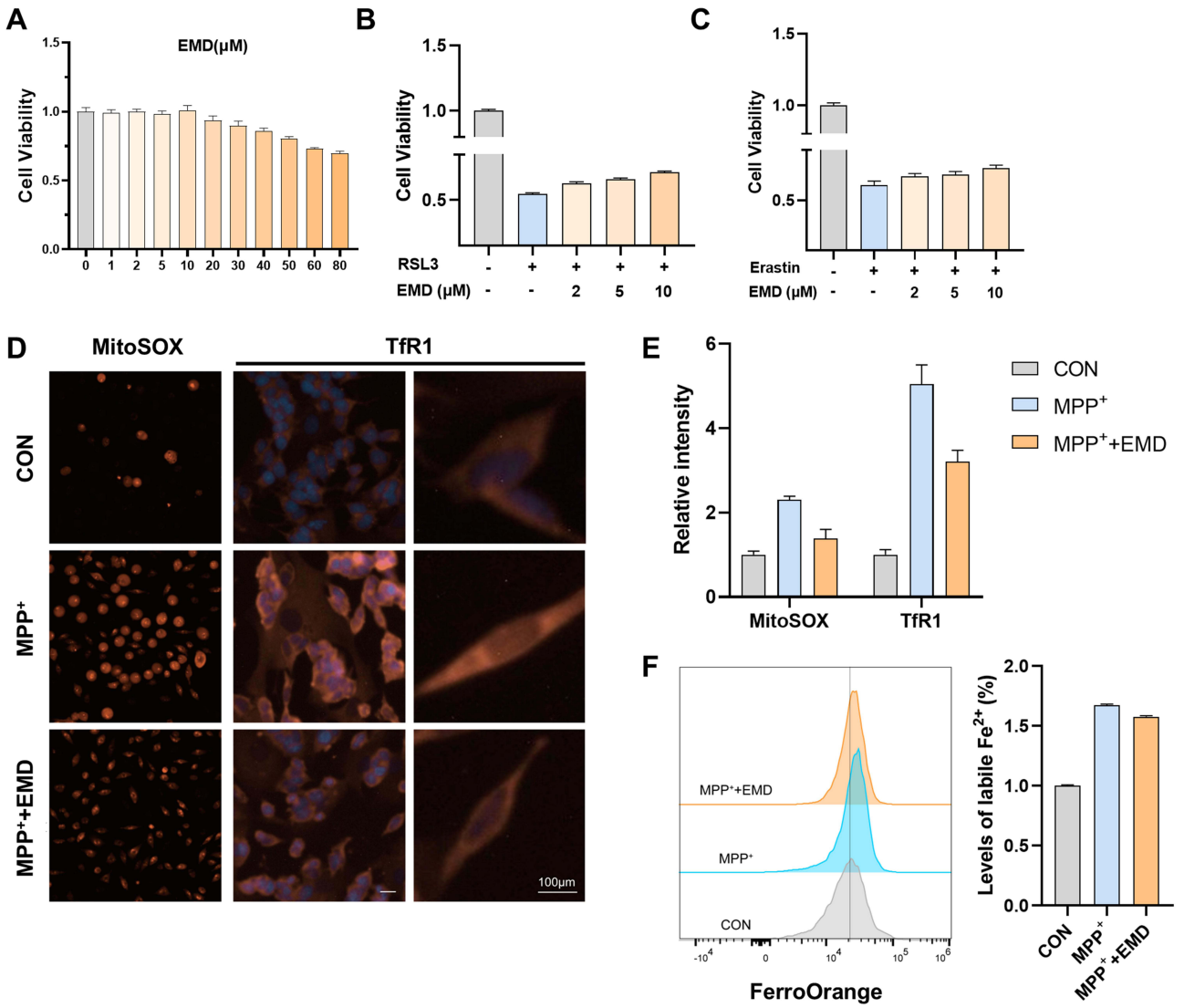

Figure 4 EMD attenuates ferroptosis induced by MPP^+ in SH-SY5Y cells. (**A**) Cell viability of SH-SY5Y under different concentrations of EMD stimulation. (**B** and **C**) Cell survival of SH-SY5Y under ferroptosis inducers insult. (**D** and **E**) Fluorescence staining for MitoSOX or TfR1 in SH-SY5Y cells. Scale bar: 100 μm. (**F**) Flow cytometry analysis revealed that EMD rescued the imbalance of iron homeostasis in MPP^+-induced SH-SY5Y cells.

upregulation of p53, TfR1, and ACSL4 protein expression (Figure 6F–I). These findings suggest that EMD protect against MPP^+-induced ferroptosis, possibly through p53 inhibition.

Discussion

The role of EMD in controlling dopaminergic neurodegeneration and its underlying mechanisms remains unclear. In this study, EMD alleviated MPTP-triggered ferroptosis, DaN cell death, and neurodegeneration in mice. Mechanistically, EMD inhibited p53 expression and suppressed the ferroptosis pathway in the midbrain of the mice. Our findings suggest that EMD may exert beneficial effects on controlling dopaminergic neurodegeneration.

EMD has been reported to exert an anti-ferroptosis effect and protects against neurodegenerative insults in mice.[22,25] Our network pharmacology analysis indicated that EMD shares 91 targets with potential PD genes, with TP53 being one of the most critical. These targets were investigated using GO and KEGG enrichment analyses. These findings indicate that EMD is associated with p53 signaling, iron-binding, and neurodegenerative diseases. Moreover, molecular docking analysis showed that EMD possibly binds to p53 and TfR1 proteins. Molecular Dynamics Simulation further confirms that the interactions between EMD and p53 remained stable over time. In animal studies, EMD treatment diminished

https://doi.org/10.2147/DDDT.S522381

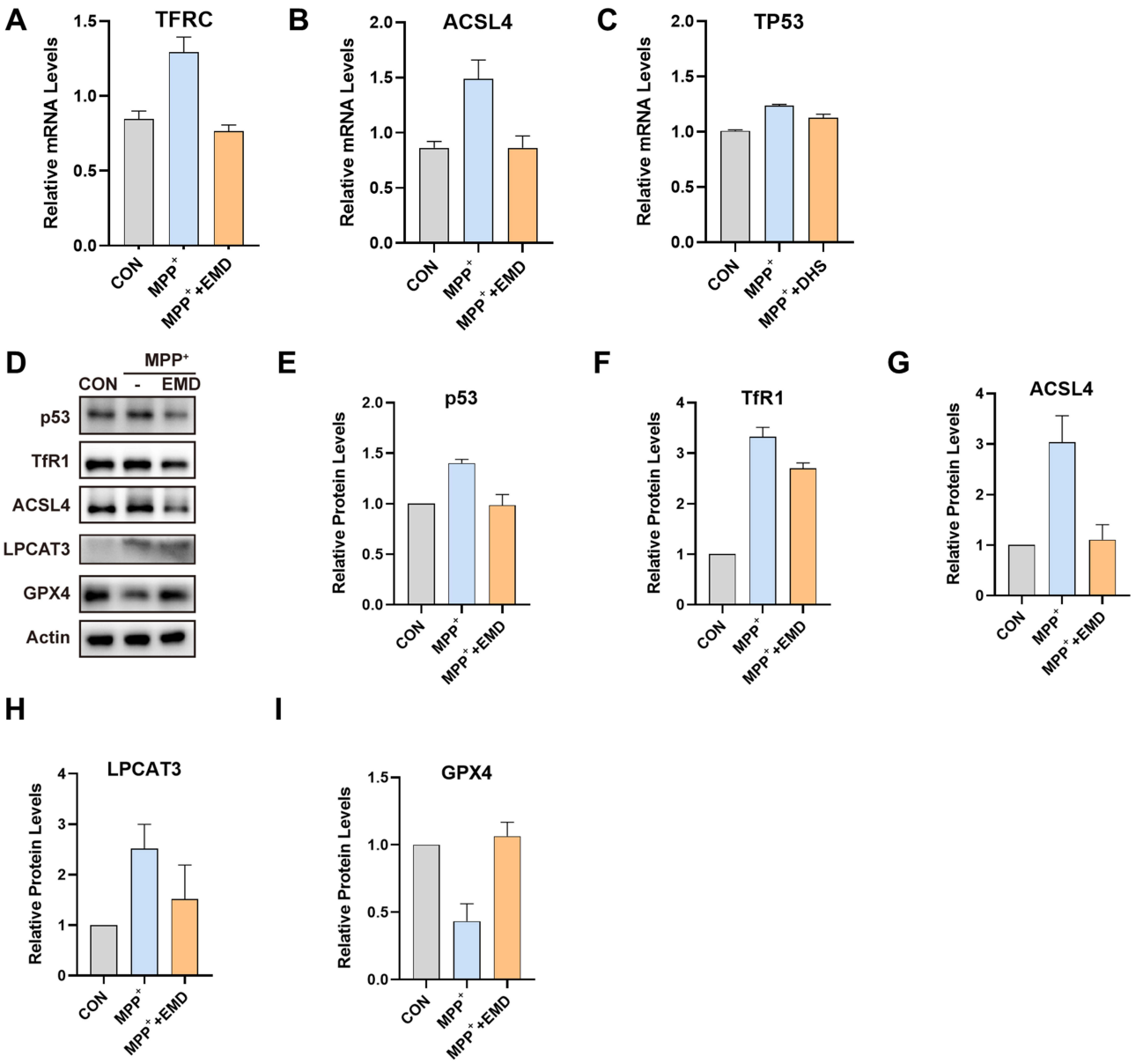

Figure 5 EMD rescues the dysregulation of p53 and curbs the ferroptosis in vitro. (**A** and **B**) Relative mRNA levels of ferroptosis-related genes in SH-SY5Y cells under MPP^+ insult. (**C**) Relative mRNA levels of TP53 in SH-SY5Y cells under MPP^+ insult. (**D–I**) Western blot assay validated that EMD effectively rescued the dysregulation of p53 and ferroptosis-related protein expression.

body weight loss in the MPTP group. A slight weight loss after MPTP injection may occur due to decreased food and water intake.[26] Treatment of high dose EMD relieved hypokinesia and neurodegeneration in mice, as evidenced by elevated total distance in open field test and rotarod test, improved SN pathologic phenotypes, and enhanced expression of TH. These findings indicate that EMD have potential therapeutic effects against neurodegenerative diseases.

It is well-established that ferroptosis in midbrain is a key factor in PD pathogenesis.[27] Inhibiting ferroptosis signaling in brain holds promise as a therapeutic strategy for PD and other brain diseases.[13] TfR1, responsible for importing iron into cells, is thought to enhance ferroptosis susceptibility by facilitating intracellular iron accumulation.[9] ACSL4, producing PUFAs to trigger ferroptosis, is a critical gene in the pathogenesis of PD.[11] We found that EMD treatment alleviated midbrain lipid peroxidation and accumulation of iron. EMD treatment decreased the expression of TFRC, ACSL4, and LPCAT3 and increased GPX4 expression in the mouse SN. Consistently, EMD treatment decreased the

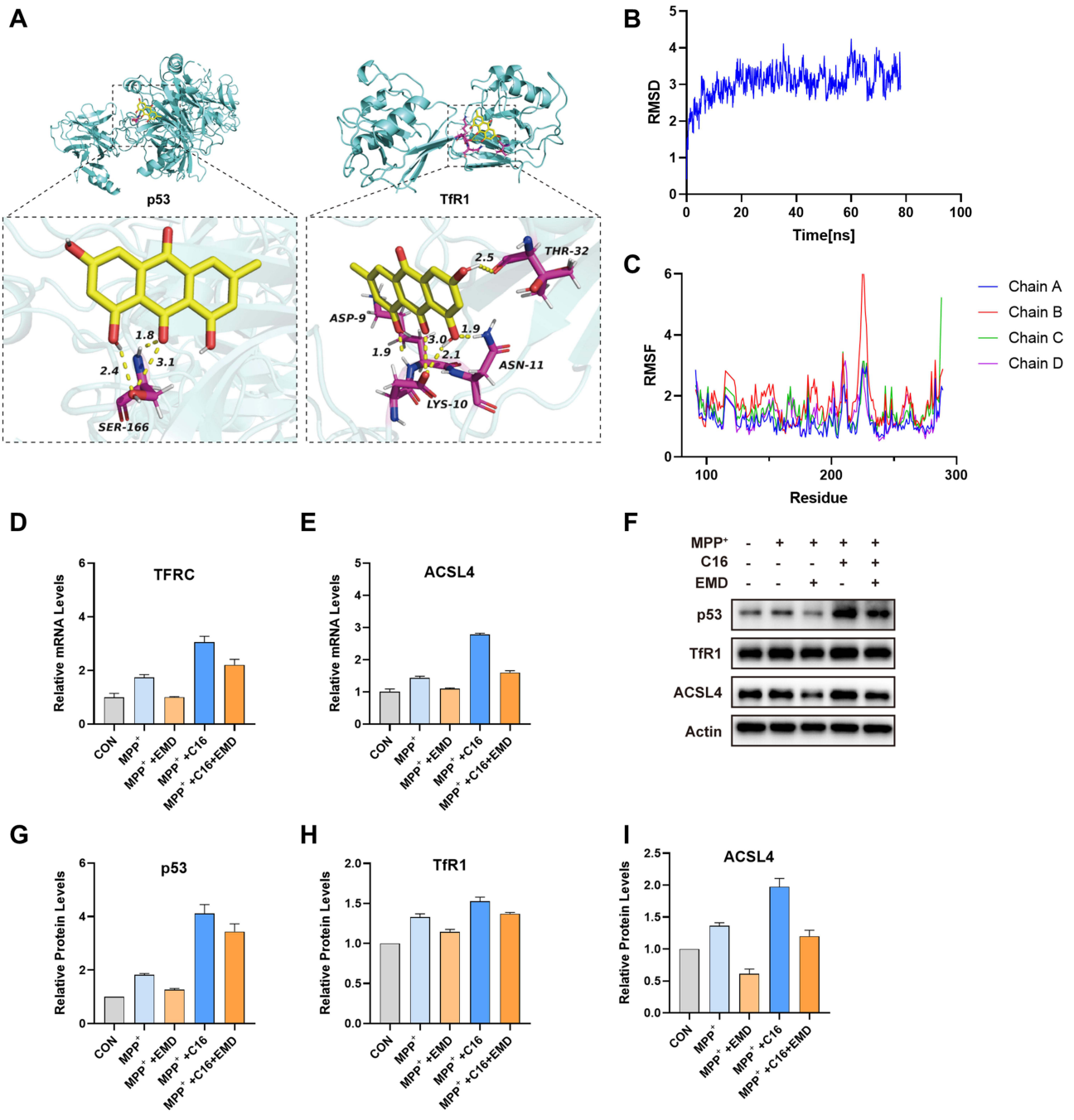

Figure 6 The activation of p53 curbs EMD inhibiting MPP^+-triggered ferroptosis in SH-SY5Y cells. (**A**) Molecular docking simulations for the binding possibility of EMD and p53 or TfR1. (**B**) RMSD plot showing the backbone stability of the protein-ligand complex over 80 ns. (**C**) RMSF plot indicating the residue-wise flexibility. (**D** and **E**) Relative mRNA levels of TFRC, and ACSL4 in SH-SY5Y cells under MPP^+ or C16 exposure. (**F**–**I**) Western blot assay validated that p53 activation attenuated the suppressive effect of EMD on ferroptosis.

protein expression of TfR1 and ACSL4 while increasing GPX4 expression in the SN of MPTP-induced mice, highlighting its protective effects against ferroptosis in dopaminergic neurodegeneration.

The p53-mediated cell death contributes to dopamine neuron loss and impairs cell survival.[28] The p53 signaling pathway regulates iron metabolism, and its imbalance disrupts cellular iron homeostasis.[18] It is reported that Ubiquitin-specific protease 7 upregulates TfR1, inducing ferroptosis via p53 activation.[29] In a brain stroke rat model, the brain undergoes ferroptosis due to increased p53 expression and decreased GPX4 activity.[30] p53 may modulate ferroptosis responses in the presence of ferroptosis inducers or high concentration ROS, suggesting that the regulation of p53 is

https://doi.org/10.2147/DDDT.S522381

potential to control ferroptosis.[17] Additionally, EMD has been reported to attenuate brain damage by suppressing p53.[31] Consistently, our findings show that EMD acts as both a p53 inhibitor and a ferroptosis modulator. Thus, we hypothesized that EMD regulates p53-ferroptosis signaling and defends against dopaminergic neurodegeneration.

In vitro, EMD suppressed the expression of TP53, TFRC, and ACSL4, while increasing the expression of FPN, GPX4, and FTH1 in SH-SY5Y cells. Similarly, EMD repressed the protein expression of p53, TfR1, and ACSL4 while increasing GPX4 levels. However, FPN expression did not increase significantly after EMD treatment, but FTH1 expression showed a slight increase, suggesting a shift toward intracellular iron sequestration rather than export. Similarly, these results were equally validated when the cells were subjected to MPP^+ insult. The alterations in gene and protein expression were almost reversed by EMD under MPP^+ conditions. These findings indicated that EMD suppressed p53 expression and regulated ferroptosis. EMD treatment improved cell survival in response to the ferroptosis inducers RSL3 and Erastin, suggesting its therapeutic potential in ferroptosis regulation. Furthermore, EMD treatment markedly inhibited cellular superoxide following MPP^+ stimulation. However, MPP^+ elevates intracellular iron, but EMD does not significantly reduce these levels. Although total cellular iron levels were not significantly reduced in vitro, the changes in ferroptosis-associated proteins and the in vivo iron reduction together support the conclusion that EMD modulates ferroptosis at least in part via iron metabolism regulation. In addition, the observation that MPP^+ simultaneously increases intracellular iron levels and TfR1 expression suggests a pathological disruption of iron regulation mechanisms. This paradoxical upregulation of TfR1 may result from MPP^+-induced oxidative stress or p53 involvement. Moreover, the EMD-induced inhibition of TFRC and ACSL4 expression was counteracted by C16. Similarly, C16 counteracted EMD-induced suppression of p53, TfR1, and ACSL4 protein expression, suggesting that EMD regulates ferroptosis signaling, possibly through p53 inhibition.

Our study has some limitations. Firstly, the small sample size ($n<5$) precludes formal statistical analysis and limits the generalizability of the findings. The results should therefore be interpreted as preliminary observations. Future studies with expanded sample size are needed to confirm these trends and explore their mechanistic basis. Secondly, the 80 ns simulation timeframe provided initial insights into ligand binding stability, longer simulations ($\geq$100 ns) would further consolidate these observations. Future studies will prioritize extended simulations using high-performance computing resources. Thirdly, our study focused on the therapeutic effects of EMD in acute MPTP-induced mice. However, the preventive effects of EMD in acute and chronic PD models require further investigation. Additionally, our research has shown that EMD curbs ferroptosis signaling by modulating the perturbation of ferroptosis molecular expression through the inhibition of p53. Although TfR1 is recognized as an upstream regulator and a hallmark of ferroptosis, further research is required to determine whether the effect of EMD on ferroptosis depends on the p53-TfR1 axis. Furthermore, we propose that the neuroprotective effects of EMD in vivo may result from its regulation of the p53-ferroptosis pathway in DaN cells. This result implicates the possible occurrence of analogous EMD events in other cells, including microglia, astrocytes, and oligodendrocytes, which probably mediate the anti-neurodegenerative effects of EMD.

Conclusions

In conclusion, our exploratory study provides preliminary evidence that EMD may be a natural regulator of the p53-ferroptosis pathway. This compound may alleviate acute MPTP-induced Parkinsonism. The potential mechanism of action of EMD may involve suppression of ferroptosis signaling in DaN via p53 inhibition. These findings suggest the potential use of EMD as a therapeutic agent in PD management.

Abbreviations

ACSL4, Acyl-CoA synthetase long-chain family member 4; C16, C16-Ceramide; CCK-8, Cell Counting Kit-8; DaN, dopaminergic neurons; DAVID, the Database for Annotation, Visualization, and Integrated Discovery; EMD, Emodin; FPN, Ferroportin1; GO, Gene Ontology; GPX4, glutathione peroxidase 4; KEGG, Kyoto Encyclopedia of Genes and Genomes; MPP^+, 1-methyl-4-phenylpyridinium; MPTP, 1-methyl-4-phenyl-1,2,3,6-tetrahydropyridine; OMIM, online Mendelian inheritance in man; PD, Parkinson's disease; PPI, protein-protein interaction; qRT-PCR, quantitative real-time polymerase chain reaction; RMSD, Root-Mean-Square Deviation; RMSF, Root-Mean-Square Fluctuation; ROS, reactive oxygen species; SEA, Similarity ensemble approach; SN, substantia nigra; Swiss, Swiss Target Prediction; TfR1, transferrin receptor 1 protein.

Acknowledgments

We thank Dr. Ling Aye for his review of the manuscript. We thank the staff of Dr. Jingcheng Dong (Huashan Hospital, Fudan University) for assistance with this study.

Author Contributions

All authors made a significant contribution to the work reported, whether that is in the conception, study design, execution, acquisition of data, analysis and interpretation, or in all these areas; took part in drafting, revising or critically reviewing the article; gave final approval of the version to be published; have agreed on the journal to which the article has been submitted; and agree to be accountable for all aspects of the work.

Funding

This research was supported by the National Natural Science Foundation of China [grant number: 82073072]. During the revision process, we performed additional Western blot experiments to strengthen our findings, which required the purchase of specific antibodies. These experimental costs were supported by: the National Natural Science Foundation of China [grant number: 82471270].

Disclosure

The authors report no conflicts of interest in this work. This paper is available as a preprint on SSRN at: https://papers.ssrn.com/sol3/papers.cfm?abstract_id=5073906.

References

1. Morris HR, Spillantini MG, Sue CM, Williams-Gray CH. The pathogenesis of Parkinson's disease. *Lancet*. 2024;403(10423):293–304. doi:10.1016/S0140-6736(23)01478-2
2. Ye H, Robak LA, Yu M, Cykowski M, Shulman JM. Genetics and pathogenesis of Parkinson's syndrome. *Annu Rev Pathol*. 2023;18:95–121. doi:10.1146/annurev-pathmechdis-031521-034145
3. Weintraub D, Aarsland D, Chaudhuri KR, et al. The neuropsychiatry of Parkinson's disease: advances and challenges. *Lancet Neurol*. 2022;21(1):89–102. doi:10.1016/S1474-4422(21)00330-6
4. Sun S, Shen J, Jiang J, Wang F, Min J. Targeting ferroptosis opens new avenues for the development of novel therapeutics. *Signal Transduct Target Ther*. 2023;8(1):372. doi:10.1038/s41392-023-01606-1
5. Xiao X, Moschetta GA, Xu Y, et al. Regulation of iron homeostasis by hepatocyte TfR1 requires HFE and contributes to hepcidin suppression in β-thalassemia. *Blood*. 2023;141(4):422–432. doi:10.1182/blood.2022017811
6. Lu LN, Qian ZM, Wu KC, Yung WH, Ke Y. Expression of iron transporters and pathological hallmarks of Parkinson's and Alzheimer's diseases in the brain of young, adult, and aged rats. *Mol Neurobiol*. 2017;54(7):5213–5224. doi:10.1007/s12035-016-0067-0
7. Ward RJ, Zucca FA, Duyn JH, Crichton RR, Zecca L. The role of iron in brain ageing and neurodegenerative disorders. *Lancet Neurol*. 2014;13(10):1045–1060. doi:10.1016/S1474-4422(14)70117-6
8. Yao Z, Jiao Q, Du X, et al. Ferroptosis in Parkinson's disease—the iron-related degenerative disease. *Ageing Res Rev*. 2024;101:102477. doi:10.1016/j.arr.2024.102477
9. Feng H, Schorpp K, Jin J, et al. Transferrin receptor is a specific ferroptosis marker. *Cell Rep*. 2020;30(10):3411–3423.e3417. doi:10.1016/j.celrep.2020.02.049
10. Ding K, Liu C, Li L, et al. Acyl-CoA synthase ACSL4: an essential target in ferroptosis and fatty acid metabolism. *Chin Med J*. 2023;136(21):2521–2537. doi:10.1097/CM9.0000000000002533
11. Tang F, Zhou LY, Li P, et al. Inhibition of ACSL4 alleviates parkinsonism phenotypes by reduction of lipid reactive oxygen species. *Neurotherapeutics*. 2023;20(4):1154–1166. doi:10.1007/s13311-023-01382-4
12. Chen X, Li J, Kang R, Klionsky DJ, Tang D. Ferroptosis: machinery and regulation. *Autophagy*. 2021;17(9):2054–2081. doi:10.1080/15548627.2020.1810918
13. Costa I, Barbosa DJ, Benfeito S, et al. Molecular mechanisms of ferroptosis and their involvement in brain diseases. *Pharmacol Ther*. 2023;244:108373. doi:10.1016/j.pharmthera.2023.108373
14. Song LM, Xiao ZX, Zhang N, et al. Apoferritin improves motor deficits in MPTP-treated mice by regulating brain iron metabolism and ferroptosis. *iScience*. 2021;24(5):102431. doi:10.1016/j.isci.2021.102431
15. Liu Y, Su Z, Tavana O, Gu W. Understanding the complexity of p53 in a new era of tumor suppression. *Cancer Cell*. 2024;42(6):946–967. doi:10.1016/j.ccell.2024.04.009
16. Song B, Yang P, Zhang S. Cell fate regulation governed by p53: friends or reversible foes in cancer therapy. *Cancer Commun*. 2024;44(3):297–360.
17. Liu Y, Gu W. p53 in ferroptosis regulation: the new weapon for the old guardian. *Cell Death Differ*. 2022;29(5):895–910. doi:10.1038/s41418-022-00943-y
18. Pan J, Xiong W, Zhang A, et al. The imbalance of p53-Park7 signaling axis induces iron homeostasis dysfunction in doxorubicin-challenged cardiomyocytes. *Adv Sci*. 2023;10(15):e2206007. doi:10.1002/advs.202206007

19. Li S, Wang M, Wang Y, et al. p53-mediated ferroptosis is required for 1-methyl-4-phenylpyridinium-induced senescence of PC12 cells. *Toxicol In Vitro*. 2021;73:105146. doi:10.1016/j.tiv.2021.105146
20. Yao Z, Jia F, Wang S, et al. The involvement of IRP2-induced ferroptosis through the p53-SLC7A11-ALOX12 pathway in Parkinson's disease. *Free Radic Biol Med*. 2024;222:386–396. doi:10.1016/j.freeradbiomed.2024.06.020
21. Hu Q, Yao J, Wu X, et al. Emodin attenuates severe acute pancreatitis-associated acute lung injury by suppressing pancreatic exosome-mediated alveolar macrophage activation. *Acta Pharm Sin B*. 2022;12(10):3986–4003. doi:10.1016/j.apsb.2021.10.008
22. Mitra S, Anjum J, Muni M, et al. Exploring the journey of emodin as a potential neuroprotective agent: novel therapeutic insights with molecular mechanism of action. *Biomed Pharmacother*. 2022;149:112877. doi:10.1016/j.biopha.2022.112877
23. Park S, Park CW, Eom JH, et al. Preclinical and dose-ranging assessment of hESC-derived dopaminergic progenitors for a clinical trial on Parkinson's disease. *Cell Stem Cell*. 2024;31(1):25–38.e28. doi:10.1016/j.stem.2023.11.009
24. Lei L, Yuan J, Dai Z, et al. Targeting the labile iron pool with engineered DFO nanosheets to inhibit ferroptosis for Parkinson's disease therapy. *Adv Mater*. 2024;36(41):e2409329. doi:10.1002/adma.202409329
25. Hu S, Zhou J, Hao J, et al. Emodin ameliorates doxorubicin-induced cardiotoxicity by inhibiting ferroptosis through the remodeling of gut microbiota composition. *Am J Physiol Cell Physiol*. 2024;326(1):C161–c176. doi:10.1152/ajpcell.00477.2023
26. Jackson-Lewis V, Przedborski S. Protocol for the MPTP mouse model of Parkinson's disease. *Nat Protoc*. 2007;2(1):141–151. doi:10.1038/nprot.2006.342
27. Liu H, Wu H, Zhu N, et al. Lactoferrin protects against iron dysregulation, oxidative stress, and apoptosis in 1-methyl-4-phenyl-1,2,3,6-tetrahydropyridine (MPTP)-induced Parkinson's disease in mice. *J Neurochem*. 2020;152(3):397–415. doi:10.1111/jnc.14857
28. Kim TW, Koo SY, Riessland M, et al. TNF-NF-κB-p53 axis restricts in vivo survival of hPSC-derived dopamine neurons. *Cell*. 2024;187(14):3671–3689.e3623. doi:10.1016/j.cell.2024.05.030
29. Tang LJ, Zhou YJ, Xiong XM, et al. Ubiquitin-specific protease 7 promotes ferroptosis via activation of the p53/TfR1 pathway in the rat hearts after ischemia/reperfusion. *Free Radic Biol Med*. 2021;162:339–352. doi:10.1016/j.freeradbiomed.2020.10.307
30. Chen C, Huang Y, Xia P, et al. Long noncoding RNA Meg3 mediates ferroptosis induced by oxygen and glucose deprivation combined with hyperglycemia in rat brain microvascular endothelial cells, through modulating the p53/GPX4 axis. *Eur J Histochem*. 2021;65(3). doi:10.4081/ejh.2021.3224
31. Guo Y, Chen Y, Zhang H, et al. Emodin attenuates hypoxic-ischemic brain damage by inhibiting neuronal apoptosis in neonatal mice. *Neuroscience*. 2024;554:83–95. doi:10.1016/j.neuroscience.2024.06.030